IMPACT DAMAGE DETECTION OF CFRP USING AN FBG ULTRASONIC SENSING SYSTEM

Hiroshi Tsuda

National Institute of Advanced Industrial Science & Technology
AIST Tsukuba Central 2, Tsukuba 305-8568, JAPAN

ABSTRACT

Impact damage of CFRP was detected using a fiber-optic ultrasonic sensing system. This fiber-optic system consists of fiber Bragg gratings for sensing and filtering, a broadband light source as well as a photo detector. Feasibility of damage monitoring using the fiber-optic system was investigated. Lamb waves generated with a piezoelectric ultrasonic transducer were propagated in a cross-ply CFRP with visible impact damage. Those waves were detected with the fiber Bragg grating sensors as well as piezoelectric sensors. Response to the Lamb wave propagated through damage area was compared with reference response in intact area. Frequency characteristics of response signal were analyzed in order to investigate the influence of damage presence on Lamb wave propagation. Experimental results showed that fiber Bragg grating sensors are comparable to piezoelectric sensors in ultrasonic detection and the fiber-optic system proved to be effective in impact damage detection of CFRP

1. INTRODUCTION

Fiber Bragg gratings (FBGs) reflect a narrowband spectral component at the Bragg wavelength when spectrally broadband light is injected into the fiber. The Bragg wavelength varies with strain applied to the FBG. Wavelength-optical intensity conversion technique has been proposed to evaluate the Bragg wavelength at high speeds. Ultrasonic wave can be detected with FBG sensors using the wavelength-optical intensity conversion technique. It is very attractive to use FBGs as ultrasonic sensors while piezoelectric devices have conventionally been used. This is because FBGs are light in weight, small size and immune to electromagnetic interference as well as easy to be multiplexed [1, 2].

In the present study, feasibility of damage detection with FBG sensor was investigated. A cross-ply CFRP with visible impact damage was used as the monitored specimen. Ultrasonic wave generated with a piezoelectric transducer was propagated in the specimen and the resultant FBG sensor response was recorded. The influence of damage on response signal behavior was investigated. Furthermore, ultrasonic wave detection with a piezoelectric sensor was performed to compare with FBG sensor response.

2. PRINCIPLE OF ULTRASONIC DETECTION USING FBGs

Propagation of ultrasonic wave in materials causes high-speed strain change in the micro strain range. High-speed strain change can be detected with FBG sensors from a wavelength-intensity conversion technique. Consider light reflected from a FBG is conducted into an optical filter whose transmissivity changes with wavelength. Then, the intensity of light transmitted through the filter depends on the Bragg wavelength of the FBG. In other words, the intensity of light transmitted through the filter depends on strain applied to the FBG. Light intensity can be measured with photo detectors. Response frequency of photo detectors is usually over 10MHz. Hence, high-speed strain change can be detected by measuring intensity of light transmitted through the optical filter using photo detectors.

In order to detect subtle strain change in the micro strain range, the optical filter must meet stringent optical characteristics whose transmissivity varies within a narrow wavelength range that includes the Bragg wavelength of the FBG sensor. FBGs seem to be suitable for the optical filter because they have very sharp wavelength characteristics whose full width at half-maximum (FWHM) is usually less than 0.5nm. Perez *et. al.* have demonstrated that an FBG sensor could detect ultrasonic waves by using an FBG as the optical filter [3].

Consider an optical system shown in Fig. 1 where the light reflected from FBG sensor is transmitted to another FBG for filtering. Light transmitted through the filter is converted into voltage signal with a photo detector. Here, we assume that the FBG sensor at strain free has a slightly longer Bragg wavelength than the FBG filter. Figure 2 shows the transmissivity of FBG filter and the change in reflectivity of FBG sensor with varying strain applied to the FBG sensor. Solid and dotted lines in the figure denote the reflectivity of the FBG sensor and the transmissivity of the FBG filter, respectively. Intensity of light reflected from the FBG sensor is represented as the area enclosed by the reflective curve. On the other hand, the light which can be transmitted through the filter is represented as the area enclosed by the transmissive curve. Therefore, the area where the reflectivity of the sensor overlaps with the transmissivity of the filter corresponds to the intensity of light transmitted through the FBG filter. In Fig. 2, the area is highlighted by shade. The Bragg wavelength of FBG sensor shifts to a shorter wavelength λ_c when the sensor is compressed. Then the overlapped area decreases, so that the intensity of light transmitted through the filter lowers. When the FBG sensor is elongated, the Bragg wavelength shifts to a longer wavelength λ_t. The overlapped area grows and the intensity of light transmitted through the filter rises. Thus, ultrasonic wave can be detected using the optical system shown in Fig. 1.

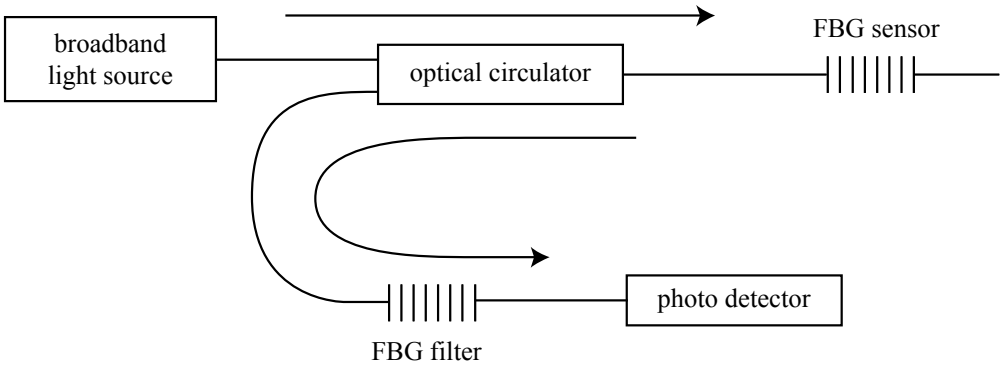

Fig. 1. FBG sensing system for ultrasonic detection.

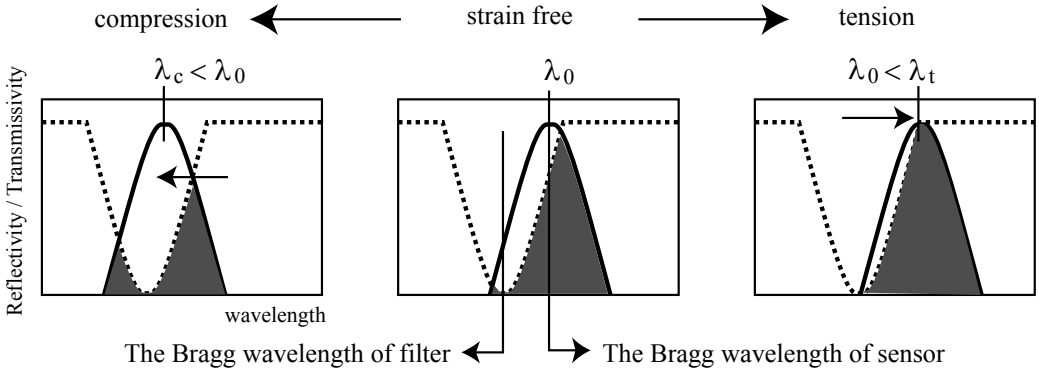

Fig. 2. A schematic illustrating the variation in photodetector output with strain applied to FBG sensor.

3. EXPERIMENTAL PROCEDURE

An experimental setup employed in the present study is shown in Fig. 3. The monitored material was a 290 X 190 X 1mm^3 carbon fiber-reinforced epoxy laminate (T800H/3631) whose fiber volume fraction was 60%. The stacking sequence was $[0/90]_{2S}$. This laminate contained an elliptically shaped 65 X 15mm^2 visible damage introduced by ball dropping. There were splitting and delamination in the damage area.

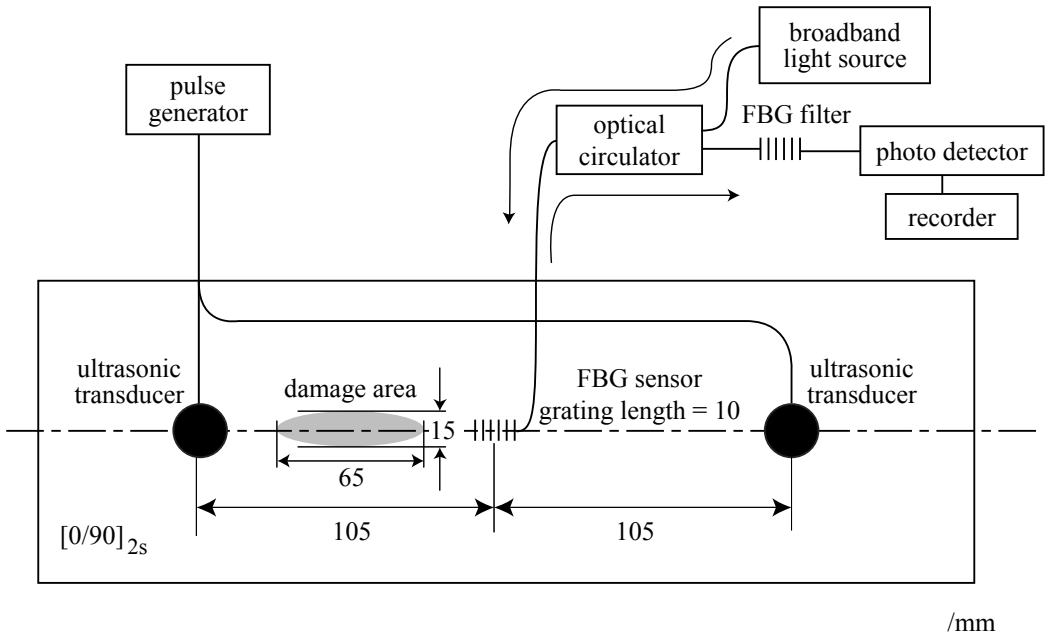

Fig. 3. A schematic of experimental setup.

Broadband light whose wavelength ranges from 1520 to 1620nm is conducted to an FBG sensor via an optical circulator. Light reflected from the sensor goes backwards through the optical circulator and then travels to an FBG filter. Light transmitted through the filter was converted into voltage signal with a photo detector. The FBG sensor was attached on the surface of CFRP using adhesive for strain gauges. Both FBGs for sensing and filtering had a grating length of 10mm, a FWHM of approximately 0.2nm and their Bragg wavelengths in strain free state were 1550.183 and 1550.173nm, respectively. Wavelength characteristics of the sensor and the filter are shown in Fig. 4.

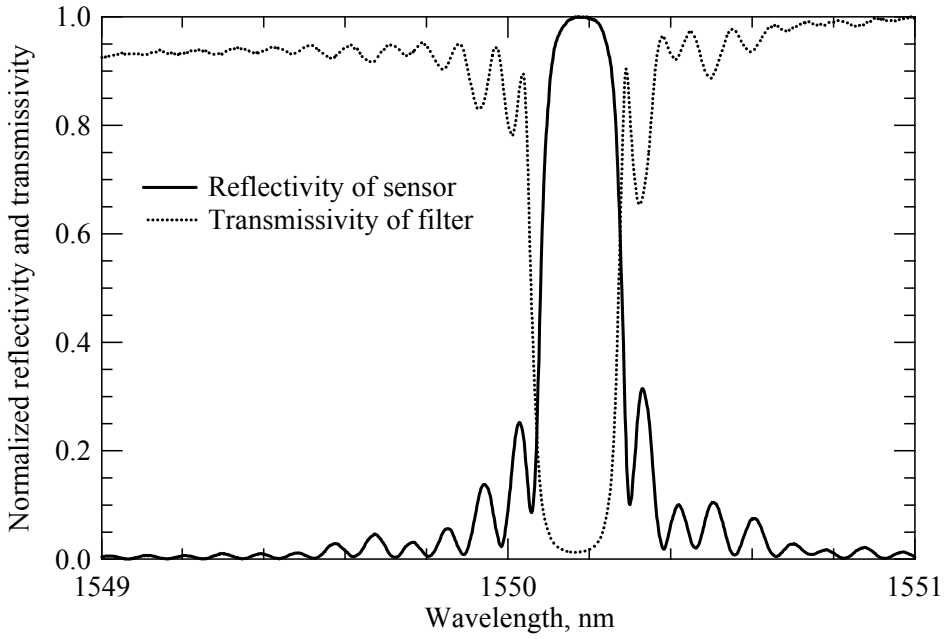

Fig. 4. Wavelength characteristics of FBGs employed.

Ultrasonic waves propagating in thin plates are referred to as Lamb waves which can be classified from the displacement with regard to the plate plane into two modes: symmetrical waves called S mode and asymmetrical waves called A mode. In a previous paper, we reported that FBG sensors were more sensitive to S mode waves than A mode waves [4]. An ultrasonic transducer that generates S mode waves was used as an ultrasonic transducer in the present study. The transducer has a diameter of 30mm and a central frequency of 250kHz. Lamb wave propagation is characterized by the product of specimen thickness and the frequency of the excitation. Only fundamental S mode waves called S_0 waves can be propagated when the product is less than 1MHz·mm [5]. The product is 0.25MHz mm under the present experimental condition, so that only S_0 waves are propagated in the specimen.

A spike signal emitted from a pulse generator was input to the ultrasonic transducer and transient Lamb wave was generated. The ultrasonic transducer was put on two places where the generated Lamb wave passed damage area or only intact area before reaching the FBG sensor. Distance between the FBG sensor and the ultrasonic transducer was 105mm. FBG response signal was recorded at a sampling rate of 100MHz and was averaged in data acquisition of 512 times.

Ultrasonic waves have conventionally been detected with piezoelectric sensors. In order to compare with the response of FBG sensor, ultrasonic Lamb wave detection with a piezoelectric sensor was performed. A piezoelectric sensor that was the same device used as the ultrasonic transmitter was attached on the same place where the FBG sensor had been attached. The piezoelectric sensor signal was recorded under the same condition as FBG sensor signal was recorded.

4. RESULTS & DISCUSSION

4.1. Response of FBG sensor to transient Lamb wave

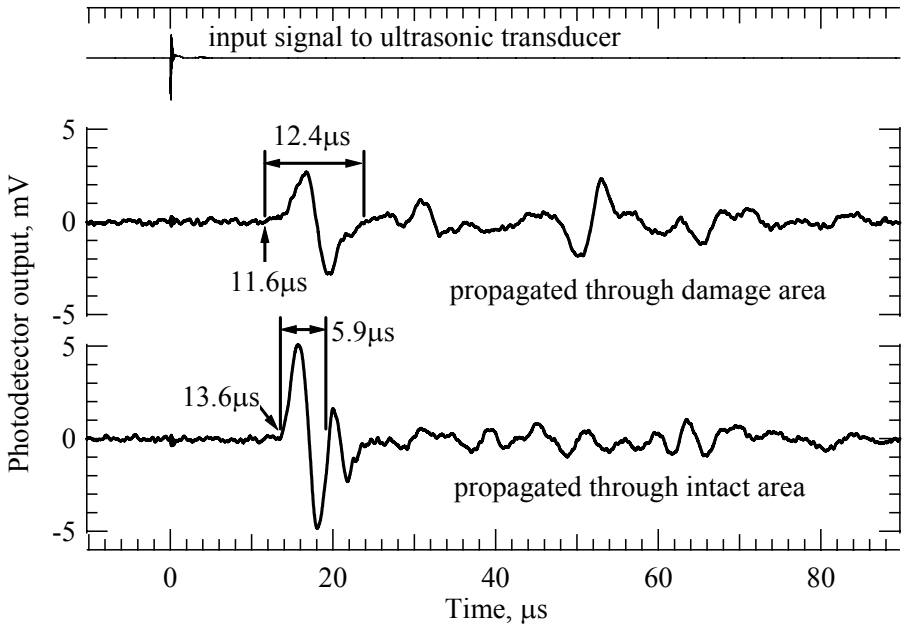

Fig. 5. FBG sensor response to Lamb wave.

FBG sensor response to transient Lamb wave propagated through either intact or damage area was shown in Fig. 5 along with the input signal to the ultrasonic transducer. A

well-defined response was demonstrated for Lamb wave propagation through intact area. The response signal rose at 13.6μs after spike signal was input to the ultrasonic transducer and the period of the first cycle was 5.9μs. The velocity of S_0 wave, V is given by Eq. (1).

$$V = \sqrt{\frac{E}{\rho}} \tag{1}$$

where E and ρ are Young's modulus and density, respectively. Unidirectional properties and density of the CFRP employed are listed in Table 1. Young's modulus of the cross-ply plate is estimated to be 83.1GPa from the rule of mixture. Using Eq. (1), S_0 wave velocity in intact area is calculated to be 7,270m/s. Then, the predicted distance of S_0 wave propagation in 13.6μs is approximately 100mm, which agrees well with the transducer-sensor interval of 105mm. This clear response proves to correspond to arrival of S_0 wave.

Table 1. Unidirectional properties and density of the CFRP employed

Longitudinal Young's modulus (GPa)	157.6
Transverse Young's modulus (GPa)	8.67
Density (kg/m^3)	1571

Response to transient Lamb wave propagated through damage area demonstrates three different features from that in intact area. First, the initial response with slight increase in amplitude starts from 11.6μs, which is 2μs earlier than the initial response in intact area. Second, the period of first cycle in response signal nearly doubles to 12.4μs. Third, intensity of response signal diminishes almost by half. The last two different features result from the wave dispersion and attenuation caused by the presence of damage.

Here, we consider why the response to Lamb wave propagated through damage area started earlier. Delamination spread over damage area of the CFRP. The 0-degree layer would separate from 90-degree layers in damage area. Consequently, Lamb wave propagation within damage area is expected to separate into 0-degree and 90-degree layers. The wave velocities in 0-degree and 90-degree layers are estimated from Eq. (1) to be 10,020 and 2,350 m/s, respectively. Then, the fastest arrival time is given by Eq. (2).

$$t = \frac{65E-3}{10,020} + \frac{40E-3}{7,300} = 12.0\mu s \tag{2}$$

The first and second terms of Eq. (2) correspond to the time to pass damage area and the rest of intact area, respectively. The predicted arrival time agrees well with the time of initial response at 11.6μs. It can be inferred, therefore, that the small response from 11.6μs would correspond to arrival of S_0 wave propagated through 0-degree layer in damage area.

Note the polarity of response. The response signal to the transient Lamb wave showed positive rising behavior. In the present experiment, the sensor had longer Bragg wavelength than the filter. It is the same Bragg wavelength condition as shown in Fig. 2 where the intensity of light transmitted through the filter increases when the FBG sensor is elongated. Hence, the FBG sensor must have been elongated by the first arrival of transient Lamb wave.

Figure 6 shows the frequency domain representation during the first cycle of response signal. The intensity of individual frequency component was normalized by the highest-intensity component. The maximum frequency components in response for intact and

damage area are 150kHz and 90kHz, respectively. The -3dB bandwidths range from 80 to 240kHz and from 50 to 160kHz, respectively. Response to Lamb wave propagated through damage area has narrower and lower frequency characteristics in comparison with response in intact area.

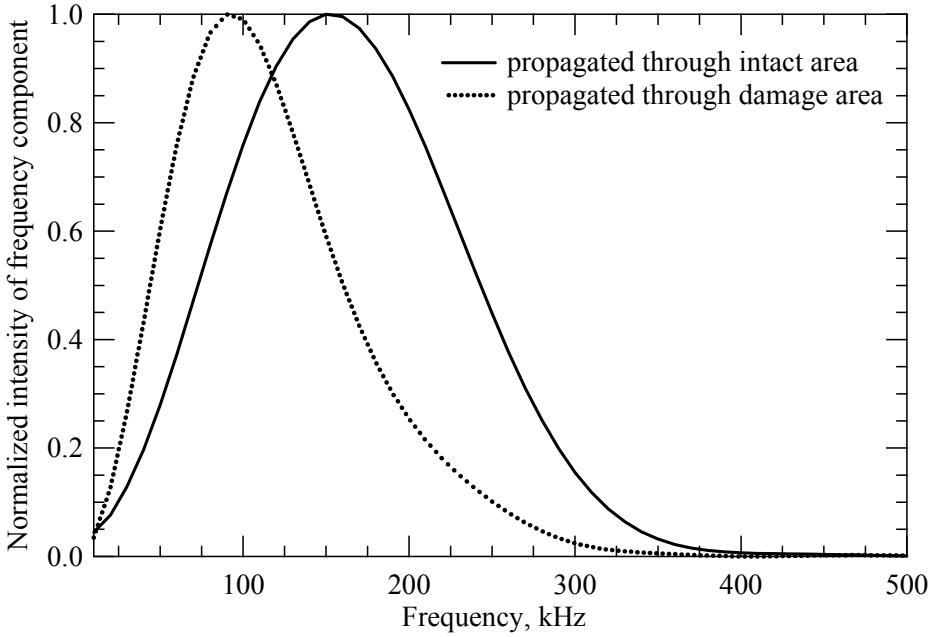

Fig. 6. Frequency characteristics during the first cycle of FBG sensor response.

4.2. Response of piezoelectric sensors

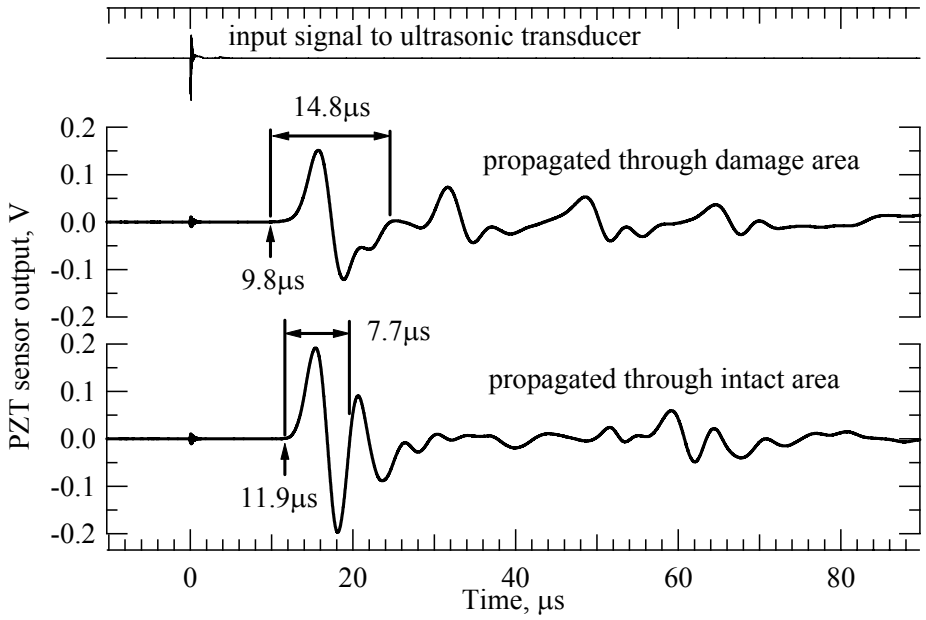

Fig. 7. PZT sensor response to Lamb wave.

Input signal to the ultrasonic transducer and corresponding piezoelectric sensor response are shown in Fig. 7. Response to Lamb wave propagated through intact area was initiated at 11.9μs and the period of the first cycle was 7.7μs. On the other hand, response to Lamb wave propagated through damage area started insignificant increase in amplitude from 9.8μs and the period of the first cycle was 14.8μs. Because of the difference in sensor size, the time of initial response and the first cycle period of piezoelectric sensor response cannot simply compare with those of FBG sensor response. However, following should be noticed. By the difference in route of Lamb wave propagation, the resultant response of piezoelectric sensor showed different behavior. The features of difference in response behavior are identical to those observed in FBG sensor response. Note the beginning of response to Lamb wave propagated through damage area, which corresponds to Lamb wave passed 0-degree layer within damage area. A piezoelectric sensor shows inconspicuous response while FBG sensor shows small but discernible response. The result proves FBG sensor to be more sensitive to Lamb wave passed 0-degree layer within damage area.

The frequency characteristics during the first cycle of piezoelectric sensor response are shown in Fig. 8. The maximum frequency components in response for intact area and damage area are 130kHz and 80kHz, respectively. The -3dB bandwidths range from 60 to 210kHz and from 40 to 130kHz, respectively. The influence of damage on the frequency characteristics of piezoelectric sensor response was identical to that observed in FBG sensors. It can be concluded from these experimental results that FBGs can work as ultrasonic sensors comparable to piezoelectric devices used conventionally.

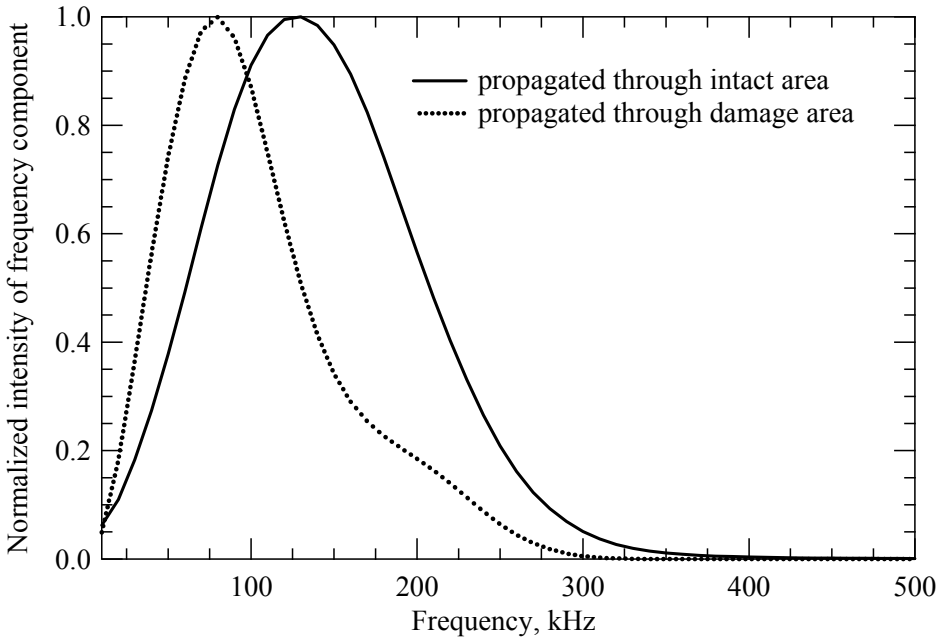

Fig. 8. Frequency characteristics during the first cycle of PZT sensor response.

5. CONCLUSIONS

An FBG sensing system for ultrasonic detection was constructed. Lamb wave generated with an ultrasonic transducer was propagated in CFRP with impact damage. FBG sensor response to Lamb wave propagated through either intact area or damaged area was recorded and analyzed. Compared with reference response in intact area, response to Lamb wave propagated through damage area showed different behavior and had narrower and lower frequency characteristics. The experimental results demonstrated that the FBG sensing system

is comparable in ultrasonic detection to conventional piezoelectric sensors and is effective for impact damage detection of CFRP.

References

1. **Kersey, A.D., et. al.,** "Fiber grating sensors", *J. Lightwave technol.* **15**/8(1997), 1442-1463.
2. **Othonos, A.,** "Fiber Bragg gratings", *Rev. Sci. Instrum.* **68**/12(1997). 4309-4341.
3. **Perez, I., et. al.,** "Acoustic emission detection using fiber Bragg gratings", *Proceedings of SPIE,* Vol. 4328, SPIE Press, (2001) 209-215.
4. **Tsuda, H. et. al.**, "Damage detection of CFRP using fiber Bragg gratings", *J. Mater. Sci. Lett.* in press.
5. **Rose, J.L.,** "*Ultrasonic waves in solid media",* Cambridge University Press, (1999), 101-131.